Proceedings of the Institute of Acoustics

EXAMINATION OF THE ACOUSTICAL PROPERTIES OF POROUS ROAD SURFACES *

Craig Howorth (1) and Keith Attenborough (2)

(1) Academic Computing Service, The Open University, Milton Keynes MK7 6AA England.
(2) Faculty of Technology, The Open University, Milton Keynes MK7 6AA England.

1. INTRODUCTION

The aim is to optimise the acoustical characteristics of the pervious macadam for noise reduction considering only the propagation (ground) effect. Other sources of road/tyre noise have been detailed by Stumpf [1]. The paper commences by describing the construction and laying of the porous road surfaces. It then maps the process of validating the microstructural model [2] as an accurate descriptor of the acoustical properties of the pervious road surface. The paper is concluded by examining the model parameters required to give the optimum linear and 'A' weighted noise reduction.

2. CONSTRUCTION OF THE FINAL TEST SURFACES

The materials were chosen to have a nominal maximum stone size grading of 20mm, 10mm and 6.3mm. Binder drainage tests were performed to determine the binder content which would ensure structural stability without significantly altering the required void content of approximately 20%. The materials resulting from these trials were laid on the test track. The normal incidence absorption coefficient was evaluated for the sample materials and the test track cores. The results indicated that the test track material was similar to that constructed in the laboratory. The test track was constructed by placing a sheet of polypropylene over a level hardcore base onto which the pervious macadam was laid. During the construction of the test track samples of the pervious material were collected and analysed by the County engineers department of Surry County Council. The test site is shown in figure 1.

* Work supported by the Transport and Road Research Laboratory whose collaboration and cooperation is gratefully acknowledged.

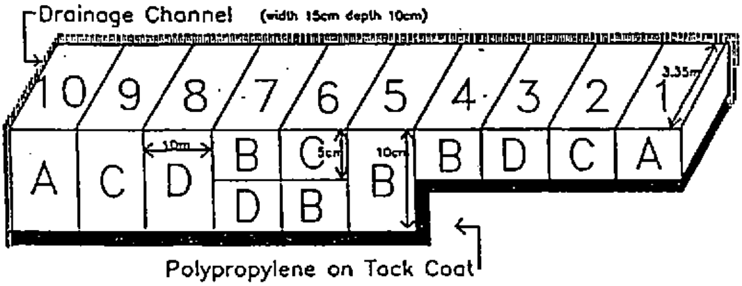

Figure 1: Diagram of test site

3 Validation of the microstructural model

The validation process involved three stages. The first stage was a series of measurements made on preliminary sites that were known to have good acoustical properties. A range of binder tests were then performed on small areas, approximately 1.0m by 1.0m to determine the binder content and a range of stone sizes. The final stage followed the construction of the test track detailed above and involved a series of measurements made on the various bays of the track, acoustical and non-acoustical measurements on cores extracted from the test track. The microstructural model developed by Attenborough [2] is proposed as a way of characterizing the acoustical properties of the road surface and the modified Weyl van der Pol formula as an adequate basis for calculating propagation effects. The study uses the indirect parameter deduction method of evaluating impedance outline by Howorth [3]. Prior to optimizing the road parameters it has to be confirmed that the model is an accurate descriptor of the acoustical characteristics of the material. This validation process is reported in four parts:

1. Acoustical procedures used for model validation
2. Non-acoustical procedures used for model validation
3. Results of point source validation process
4. Extension to validation using vehicle source

3.1 Acoustical procedures used for model validation

Two acoustical techniques are employed the data from which is used with a minimization technique in order to deduce the microstructural model parameters. These parameters are then compared to those deduced from non–acoustical measurements.

3.1.1 Level difference measurements

The sound field above a surface is measured by a pair of vertically separated receivers at a short range from a point source. The lower microphone is positioned close to the surface, figure 2.

A white noise source is used and the level difference spectrum is found from;

$$L.D. = 20.\log\left(\frac{p_2}{p_1}\right) \tag{1}$$

where p_n is the modulus of the pressure at receiver position n. The lower microphone acts as a measure of the direct field if the source is conically symmetrical, i.e. the ray amplitude traced along the path R_{11} is the same as that travelling along R_{12}, as described by Embleton [4]. Thus the level difference spectrum is independent of the frequency response and any variations in the power of the acoustic source.

3.1.2 Normal incidence absorption coefficient data

The standing wave tube technique was used to measure the normal incidence impedance and absorption coefficient of a number of core samples taken from the test sites. The cores either 94mm or 97mm in diameter were taken following the level difference measurements from the point of specular reflection. This lies midway between the source and receiver array if the upper microphone is at the same height as the source. This method of core collection should ensure that the non-acoustical measurements are carried out on a core from the area examined by the level difference technique. For the latter measurements a 97mm core was chosen as standard as this was the internal diameter of the standing wave tube used to collect the impedance data.

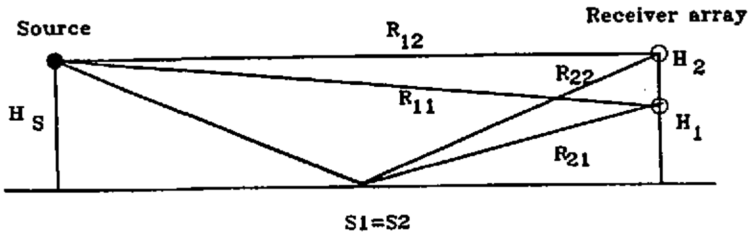

Figure 2: Level difference geometry

3.2 Non–acoustical measurements

3.2.1 Layer depth

The layer depth was measured directly on the core samples taken from the road surface. This was aided by laying the test track material onto a polypropylene layer.

3.2.2 Flow resistivity

The flow resistivity was measured on the test cores using an air flow rig. Compressed air regulated by a series of valves passes through a narrow tube to a small chamber. The motion of the air produces a partial vacuum which is filled by air being drawn through the sample. The rate of flow is controlled by a series of meters and may range from 8.7 litres/minute to 0.1 litres/minute. A pair of micromanometers measure the pressure drop across the surface with respect to the atmospheric pressure for each flow rate. resistivity is calculated from equation 2.

$$R = \frac{C_1 A \Delta P}{Q L} \qquad (2)$$

where

R the flow resistivity in MKS Rayls/m

L the length of the sample in cm

Q the flow rate in cm^3/sec

ΔP the pressure drop in inches H_2O

C_1 is a conversion factor equal to 2490000 for the above units

3.2.3 Porosity

The porosity is defined at the ratio of the volume of inter-connected air space to the volume of the sample. The porosity of the material was evaluated using a water saturation technique.

3.2.4 Tortuosity

The tortuosity of a porous material is a measurement of the increased path length through the material due to the deviation from a straight line. It is possible to relate the tortuosity of a sample to the electrical conductivity of a conductive fluid saturated material. The electrical resistance increases as the pores become more tortuous and the path length between the electrodes increases. A method has been proposed by Champoux et al [5] which compares the conductivity of a sample saturated with saline to that of the saline solution.

3.3 Results of the point source validation process

Table 1 to 3 summarize the microstructural model parameters deduced both acoustically and non-acoustically for the test bays.

Parameter/Site	Material A 20mm hf	Material B 20mm nf	Material C 10mm	Material D 6mm
5cm level diff fit				
Flow resistivity	1976	1653	3743	11922
Porosity	0.28	0.287	0.238	0.19
Grain shape	0.74	0.497	0.75	0.62
(Tortuosity)	(2.56)	(1.85)	(2.93)	(2.80)
Pore shape	0.86	0.61	0.48	0.58
Layer depth	0.059	0.062	0.0609	0.0619
10cm level diff fit				
Flow resistivity	1625	1680	3270	32500
Porosity	0.290	0.292	0.234	0.146
Grain shape	1.27	0.859	1.03	1.12
(Tortuosity)	(4.81)	(2.87)	(4.46)	(8.62)
Pore shape	1.41	0.477	0.739	0.85
Layer depth	0.114	0.0984	0.11	0.105
Double layer fit				
Flow resistivity		1653	3750	11900
Porosity		0.237	0.254	0.190
Grain shape		0.497	0.77	1.00
(Tortuosity)		(2.04)	(2.87)	(5.26)
Pore shape		0.51	0.48	1.5
Layer depth		0.06	0.065	0.041

Table 1: Parameters deduced from test track via level difference fitting

Note: hf and nf are used as abbreviations for normal flakiness and high flakiness.

Parameter/Site	Material A 20mm hf	Material B 20mm nf	Material C 10mm	Material D 6mm
5cm absorption coeff fit				
Flow resistivity	1970	1670	3250	11900
Porosity	0.282	0.287	0.235	0.193
Grain shape	1.35	0.89	0.96	1.13
(Tortuosity)	(5.52)	(3.03)	(4.01)	(6.41)
Pore shape	0.83	0.58	0.47	0.55
Layer depth	0.058	0.061	0.061	0.062
10cm absorption coeff fit				
Flow resistivity	1425	1830	3270	33500
Porosity	0.285	0.255	0.238	0.146
Grain shape	1.21	0.954	1.03	1.09
(Tortuosity)	(4.56)	(3.66)	(4.38)	(8.14)
Pore shape	1.17	0.577	0.539	0.52
Layer depth	0.114	0.105	0.105	0.105
Double layer absorption coeff fit				
Flow resistivity		1650	3743	11000
Porosity		0.29	0.238	0.20
Grain shape		0.89	0.97	1.14
(Tortuosity)		(3.00)	(4.02)	(6.26)
Pore shape		0.50	0.48	0.48
Layer depth		0.060	0.058	0.061

Table 2: Parameters deduced from test track via absorption coefficient fitting

Note: hf and nf are used as abbreviations for normal flakiness and high flakiness.

Parameter/Site	Material A 20mm hf	Material B 20mm nf	Material C 10mm	Material D 6mm
Measured 94/5				
Flow resistivity	1900	1640	3600	11450
Porosity	0.229	0.255	0.242	0.210
Grain shape	1.37	0.89	0.97	1.14
(Tortuosity)	(7.53)	(3.77)	(3.96)	(5.92)
Pore shape				
Layer depth	0.055	0.0615	0.059	0.060
Measured 97/5 (1)				
Flow resistivity	1425	1475	3700	10800
Porosity	0.283	0.293	0.243	0.208
Grain shape	1.17	0.91	1.14	1.16
(Tortuosity)	(4.41)	(3.07)	(5.04)	(6.21)
Pore shape				
Layer depth	0.055	0.0615	0.062	0.060
Measured 97/10 (1)				
Flow resistivity	1550	1525	3300	33500
Porosity	0.229	0.255	0.242	0.146
Grain shape	0.90	0.91	0.96	N/A
(Tortuosity)	(3.80)	(3.51)	(3.91)	(N/A)
Pore shape				
Layer depth	0.12	0.10	0.11	0.105
Measured 97/5 (2)				
Flow resistivity	1565	1670	3200	9200
Porosity	0.261	0.208	0.305	0.208
Grain shape	1.13	0.85	1.32	1.08
(Tortuosity)	(4.61)	(3.83)	(4.81)	(5.52)
Pore shape				
Layer depth	0.060	0.057	0.058	0.060
Measured 97/10 (2)				
Flow resistivity	1360	1785	3450	34750
Porosity	0.279	0.277	0.262	0.127
Grain shape	N/A	1.06	1.04	0.89
(Tortuosity)	(N/A)	(3.91)	(4.03)	(6.39)
Pore shape				
Layer depth	0.099	0.095	0.098	0.112

Table 3: Parameters deduced from test track via non-acoustical measurements

3.4 Extension to validation from vehicle sources

As the results from the point source measurements indicate that the microstructural model is an accurate description of the acoustical properties of the material under study the validation process was extended to included noise from a vehicle source. Two vehicles were employed; an estate car and a H.G.V. tractor unit. The level difference spectra for each vehicle was modelled as an array of point sources. The data was used to evaluate the impedance model parameters using the minimization technique. The results are shown in table 4

Parameter	Material	Material	Material	Material
Car	A	B	C	D
Flow resistivity	1976	1600	3743	11922
Porosity	0.23	0.26	0.22	0.18
Grain shape	0.79	0.69	0.68	0.62
(Tortuosity)	(3.19)	(2.53)	(2.79)	(2.89)
Pore shape	0.90	1.49	0.90	0.88
Layer depth	0.059	0.0625	0.063	0.61
H.G.V.	A	B	C	D
Flow resistivity	1970	1640	3600	11800
Porosity	0.21	0.25	0.21	0.18
Grain shape	0.87	0.85	0.9	1.0
(Tortuosity)	(3.88)	(3.24)	(4.07)	(5.55)
Pore shape	1.7	0.9	0.8	0.5
Layer depth	0.048	0.055	0.055	0.05

Table 4: Parameters deduced from vehicular source tests, sites 1 to 4

4 Surface optimization

Having validated the applicability of the microstructural model and the modified Weyl van der Pol approximation for point and vehicle sources the model may now be used to find the acoustic properties of the road surfaces that should give optimum noise reduction (considering only the propagation effect). The linear and 'A' weighted noise reductions were evaluated for a series of situations.

4.1 Results of optimization procedure

The optimization procedure is divided into seven sections

1. Optimization presuming total independence of the microstructural model parameters.
2. Optimization assuming the Bruggeman relationship is a valid relationship between the porosity and tortuosity.
3. Optimization assuming the Bruggeman relationship and the modified Carman relationship relating flow resistivity to porosity and tortuosity is valid.
4. Optimization presuming total independence of the microstructural model parameters and an extended source.
5. Suggested surfaces for optimum noise reduction.
6. Optimization between a range of pervious road surfaces and three tyre tread patterns for light vehicles.
7. Optimization between a range of pervious road surfaces and three tyre tread patterns for heavy vehicles.

The results of stages 1 to 4 suggested a high porosity material that would not be structurally viable. Thus seven feasible surfaces have been studied. It appears that a thick (i.e. superthick, a large thickness compared to the 5cm deep layers laid on most road surfaces) layer of low flow resistivity (1500 MKS Rayls) material would be most suitable for reducing most vehicular noise. An alternative surface is provided by placing a layer of low flow resistivity material upon a small grained surface with a flow resistivity of 30000 MKS Rayls. The study of tyre tread types indicates again that the 'superthick layer' is the preferred surface for all tyre types. There does not appear to be any optimum combination of tyre and road surface for either light or heavy vehicles.

REFERENCES

[1] H.W. Stumpf. Linking evaluation of heavy truck tyre noise, measured by iso 362, with scale factors for sound intensity. In *International tire/road noise conference*, 1990.

[2] K. Attenborough. Acoustical characteristics of porous materials. *Physics Reports*, 1981.

[3] Howorth C. *Sound Propagation Over Rigid Porous Layers*, PhD thesis, The Open University, Walton Hall, Milton Keynes, England, 1991.

[4] T.F.W. Embleton, J.E. Piercy, and G.A. Daigle. Effective flow resistivity of ground surfaces determined by acoustical measurements. *Journal of the Acoustical Society of America*, 74(4): 1239-1244, 1983.

[5] Champoux Y. and Stinson M.R. Measurement of tortuosity of porous materials and the implications for acoustic modelling. In *Proceeding of the Acoustical Society of America*, 1990. Supplement 1 (87).